Available online at www.sciencedirect.com
SCIENCE DIRECT®
Journal of Sound and Vibration 286 (2005) 363–381
JOURNAL OF SOUND AND VIBRATION
www.elsevier.com/locate/jsvi

Short Communication

Analyses of radiation impedances of finite cylindrical ducts

W. Shao, C.K. Mechefske*

Department of Mechanical Engineering, Queen's University, Kingston, Ont., Canada K7L 3N6

Received 22 September 2003; received in revised form 3 November 2004; accepted 18 November 2004
Available online 26 January 2005

Abstract

To aid in understanding the characteristics of acoustic radiation from finite cylindrical ducts with infinite flanges, mathematical expressions of generalized radiation impedances at the open ends have been developed. Newton's method is used to find the complex wavenumbers of radial modes for the absorption boundary condition. The self-radiation impedances and mutual impedances for some acoustic modes are calculated for the ducts with rigid and absorption walls. The results show that the acoustical conditions of the duct walls have a significant influence on the radiation impedance. The acoustical interaction between the two open ends of the ducts cannot be neglected, especially for plane waves. To increase the wall admittance will reduce this interference effect. This study creates the possibility for simulating the sound field inside finite ducts in future work.

1. Introduction

A magnetic resonance imaging (MRI) scanner provides high-resolution spatial images of biological subjects and has become one of the most widely used diagnostic devices in the health care and medical research field. Anyone who takes an MRI examination may feel uncomfortable because of the high-intensity acoustic noise inside the bore of MRI scanner, which can reach 120 or 130 dB (A) [1,2]. The noise is mainly produced by the vibration of the so-called gradient coils, which are bound together as a cylindrical duct [3].

*Corresponding author. Tel.: +1 613 533 3148; fax: +1 613 533 6489.
E-mail address: chrism@me.queensu.ca (C.K. Mechefske).

0022-460X/$ - see front matter © 2004 Elsevier Ltd. All rights reserved.
doi:10.1016/j.jsv.2004.11.017

A mathematical model for the acoustic radiation from MRI scanners was first developed by Kuijpers [4], who presented a model of baffled finite ducts to describe the acoustic radiation of the gradient coils. He derived a semi-analytical formulation for the acoustic radiation of a finite duct with open ends mounted with infinite flanges. The acoustic field inside the duct was described with Fourier–Bessel modes. The radiation of acoustic waves at the duct's exit was described with generalized radiation impedance.

In duct acoustics, radiation from infinite ducts with rigid walls is well understood [5,6]. On the other hand, the sound field inside finite ducts is difficult to calculate because of reflections of acoustic waves at the open ends. Dock [7,8] discussed the effects of duct cross-section geometry, source distribution space–time patterns and the termination conditions to the sound field in hard-walled ducts of finite length. In his analyses, identical source distributions produced different sound fields in infinite and finite ducts.

Because the acoustic radiation impedances at the opening of ducts influence both the inside and outside sound field, they have attracted considerable interest from researchers in this field. Morse [9] had calculated the plane wave radiation impedance for a circular opening. Felsen and Yee [10] used the Ray method to calculate the modal reflection and coupling coefficient for flanged and unflanged semi-infinite hard-wall circular tubes for the plane wave mode. Mofrey [11] presented calculations of radiation efficiency of acoustic modes in a baffled annular opening. His results showed that the variation of radiation efficiency with frequency can be generalized in terms of mode cut-off. Based on a Helmholtz integral of acoustic radiation for the open end of a duct, Zorumski [12] extended previous work by deriving the formula of generalized radiation impedances for semi-infinite circular and annular ducts with an infinite flange and finite wall acoustic admittance. An infinite-matrix equation was used to describe the relationship between the mode reflection and impedance at the opening. Results showed that the boundary condition of walls was a significant parameter to decide the radiation impedance. However, these investigations were restricted to situations where ducts were of semi-infinite in length. When a sound radiator is operating in the close proximity with other radiators, the performance of each unit may be affected by their acoustic interaction [13]. This requires that the interaction of both openings should be taken into consideration if the duct is finite in length and it can be described in terms of mutual radiation impedances.

To the authors' knowledge, no studies have been reported in the literature dealing with the acoustical interaction between the openings of finite ducts with rigid and absorption boundary conditions, although much work was done on the mutual impedance for radiators in semi-infinite planes. Sherman [14] derived the expressions for the mutual radiation impedance for uniformly vibrating circular and rectangular acoustic sources on a rigid spherical baffle. Greenspon and Sherman [15] calculated the mutual impedance for pistons in a cylinder. The mutual acoustic impedances of radiators and flexible disks in an infinite rigid plane were investigated by Pritchard [13] and Chan [16], respectively. The self- and mutual-impedances of uniformly vibrating pistons of various shapes in an infinite rigid plane were calculated by Thompson [17].

Acoustic wave propagations in ducts are quite different from the sound radiation in free fields or semi-infinite fields. Thus the theories used in the above references cannot be directly applied for the computation of the mutual radiation impedance for finite ducts. Although Johnston and Ogimoto [18] found that the small oscillations in the impedance at openings for a finite-length duct compared with that for a semi-infinite length duct and Wang and Tszeng [19] investigated the

effects of acoustical interference to the radiation impedance, reflection coefficient and the far-field radiation pattern between two ends of a finite duct for some simple situations, they did not give detailed mathematical expressions to describe the mutual impedance.

Since most work has dealt with the radiation problem for hard-walled semi-infinite cylindrical ducts, mathematical expressions for calculating radiation impedance for flanged finite ducts with rigid and absorption walls are presented here. These are the extensions of the models developed by Zorumski [12] and Kuijpers [4]. The self-radiation impedances and mutual radiation impedances are calculated for some least-attenuated modes (normally lower orders) because these modes determine the sound reduction under general conditions of excitation [6]. The Newton method is used to find the complex wavenumbers of radial modes for absorption walls. This study provides a base for computations of the sound field inside the finite ducts.

2. Theoretical models

Formulas for the radiation impedances at the openings of flanged finite cylindrical ducts will be derived in this section. First, the acoustic model for cylindrical ducts is briefly reviewed. Then the expression for self-radiation impedance will be presented, as there will be the reflection of acoustic waves at the opening of ducts. Finally, the equations for the mutual radiation impedance will be derived.

2.1. Acoustical models for cylindrical ducts

In order to describe the sound radiation of flanged finite cylindrical ducts with constant circular cross-section, the theoretical model of generation and propagation of sound waves in such ducts should satisfy some conditions [20]: the acoustic pressure, density and velocity must satisfy appropriate wave equations; the pressure and the displacement of the fluid in the normal direction near the duct walls must equal those on contacting boundaries of the duct walls; the pressure and displacement fields on the source side and the fluid side must be continuous. Waves reflecting from walls interfere with each other, giving interference patterns (similar to standing waves) over the cross-section.

The acoustic field inside the duct without any source is determined by the Helmhotz equation

$$\nabla^2 p + k^2 p = 0, \tag{1}$$

where ∇^2 is the Laplacian ($\nabla^2 = \partial^2/\partial x^2 + \partial^2/\partial y^2 + \partial^2/\partial z^2$), p is the acoustic pressure in the sound field and k is the wavenumber which is equal to ω/c (ω is the frequency, c is the speed of sound) in the free field. The selection of cylindrical polar coordinates x, r, θ is made for convenience when solving a problem in a cylindrical duct and the Laplacian term is then [20]

$$\nabla^2 = \frac{\partial^2}{\partial x^2} + \frac{1}{r}\frac{\partial}{\partial r}\left\{r\frac{\partial}{\partial r}\right\} + \frac{1}{r^2}\frac{\partial^2}{\partial \theta^2}, \tag{2}$$

where x is the coordinate in the axial direction of the duct, r is in the radial direction and θ is in the circumferential direction (see Fig. 1). A modal solution of this equation is (a time factor $e^{i\omega t}$ is

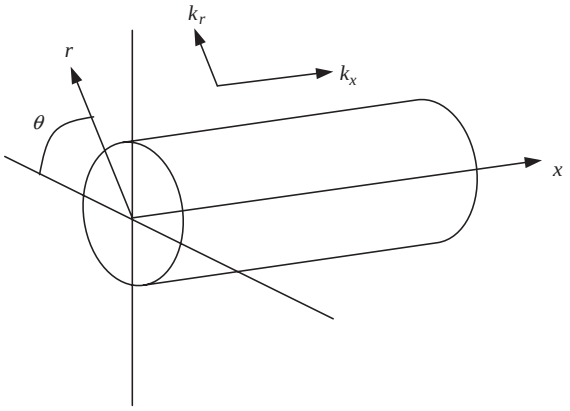

Fig. 1. Cylindrical polar coordinates.

understood throughout this paper)

$$p(r,\theta,x)=\sum_{m=-\infty}^{\infty}\sum_{n=1}^{\infty}J_m(k_r^{mn}r)\mathrm{e}^{-\mathrm{i}m\theta}[A_{mn}\mathrm{e}^{-\mathrm{i}k_x^{mn}x}+B_{mn}\mathrm{e}^{\mathrm{i}k_x^{mn}x}], \tag{3}$$

where $J_m(k_r r)$ is the Bessel function of the first kind of order m. It gives the position of nodal lines of the pressure in the radial direction. A and B are the modal coefficients of the forward-propagating and backward-propagating acoustic wave modes respectively. k_x and k_r are the wavenumbers in the axial and the radial direction respectively (see Fig. 1); m is the number of circumferential modes in the harmonic complex pressure amplitude and n is the number of radial modes.

For a hard-walled cylindrical duct, the boundary condition $\partial p/\mathrm{d}r=0$ at $r=a$ (a is the radius of the cylindrical duct) is required. The wavenumbers of radial modes can be obtained from the roots of the eigenequation $\mathrm{d}[J_m(k_r r)]/\mathrm{d}(k_r r)=0$. For a certain order m, there exists a series of roots (n is used to represent the nth root). The wavenumbers of radial and axial wave modes must satisfy the acoustic wave equation [5]

$$(k_x^{mn})^2+(k_r^{mn})^2=k^2 \tag{4}$$

when at a particular frequency, the axial wavenumber $k_x^{mn}=\sqrt{k-k_r^{mn}}=0$. This is called the cut-off frequency below which the particular modes cannot propagate freely in the duct. Those axial modes above the cut-off frequency are called cut-on modes.

On the other hand, if the duct walls are not rigid but locally reactive to the pressure, the boundary condition can be defined by an acoustic impedance $Z=p/u_n$ or a specific acoustic admittance could be defined as $\beta=\xi-\mathrm{i}\sigma=\rho c/Z$ [6], where p is the pressure on the surface, u_n is the normal surface velocity; ρ and c are the density and sound speed of the media respectively. Thus the boundary is

$$\frac{\partial p}{\partial n}=\mathrm{i}k\beta p. \tag{5}$$

Then, the Bessel functions should satisfy [6, p. 510]

$$k_r^{mn} J'_m(k_r^{mn} a) = \mathrm{i}\beta k J_m(k_r^{mn} a). \tag{6}$$

When the wall admittance is comparatively small ($|\beta|ka|$ is considerably smaller than unity), the approximate solution is

$$\begin{aligned} k_r^{01} &= -\mathrm{i}\sqrt{2(\mathrm{i}\beta ka)} \quad (\textit{plane waves}), \\ k_r^{mn} &= q_r^{mn}\left(1 - \frac{(\sigma + \mathrm{i}\xi)ka}{(q_r^{mn}a)^2 - m^2}\right), \quad (m \neq 0,\ n \neq 1), \end{aligned} \tag{7}$$

where q_r^{mn} is the wavenumber of the acoustic modes for rigid boundary conditions. k_r^{mn} are generally complex, so the axial wavenumbers k_x^{mn} are also complex. Their imaginary parts then determine the axial decay rates for the cut-on modes. If $|\beta|ka|$ is not small, the k_r^{mn} should be calculated by numerical methods using Eq. (6).

2.2. Generalized self-radiation impedance

Acoustic waves propagating in a finite duct cannot go totally through its termination apertures. Only a part of the acoustic energy can radiate from the open ends of the duct and the other part will be reflected. This phenomenon is described in Fig. 2, where the P^+, P^- and P' are the incident wave, reflected wave and transmission wave (radiating out the duct), respectively.

The acoustic pressure and velocity amplitudes at the open ends of the duct can be expressed in terms of the acoustic modes in radial r and circumferential θ directions as

$$p(r, \theta, x) = \sum_{m=-\infty}^{\infty} \mathrm{e}^{-\mathrm{i}m\theta} \sum_{n=1}^{\infty} P_{mn} J_m(k_r^{mn} r), \tag{8}$$

$$u_x(r, \theta, x) = \frac{1}{\rho c} \sum_{m=-\infty}^{\infty} \mathrm{e}^{-\mathrm{i}m\theta} \sum_{n=1}^{\infty} V_{mn} J_m(k_r^{mn} r), \tag{9}$$

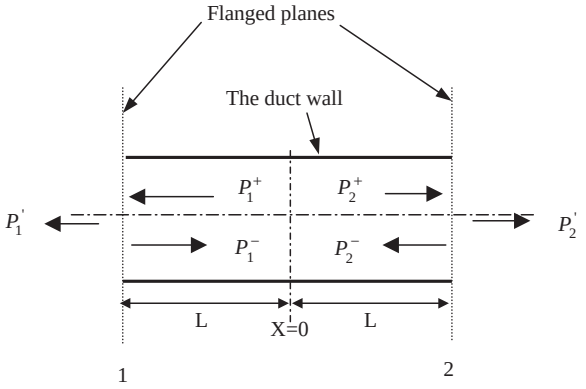

Fig. 2. The reflection at the open ends of cylindrical ducts.

where P_{mn} and V_{nm} are the modal coefficients for the pressure and velocity respectively. Zorumski [12] introduced the concept "generalized radiation impedance Z'" for a semi-infinite duct with an infinite flange to describe the relation between the modal pressure and velocity amplitudes, which could be used as the generalized self-radiation impedance for a finite duct:

$$P_{mn} = \sum_{l=1}^{\infty} Z'_{mnl} V_{ml}, \tag{10}$$

where l and n are the orders of radial incident and reflected modes respectively. Thus generalized radiation impedance can be written as

$$Z'_{mnl} = \frac{-\mathrm{i}}{N_{mn}N_{ml}} \int_0^{\infty} \frac{\tau}{\sqrt{\tau^2 - 1}} D_{mn}(\tau) D_{ml}(\tau)\, \mathrm{d}\tau, \tag{11}$$

$$N_{mn} = ka \left[\frac{1}{2} \frac{((k_r^{mn}a)^2 - m^2) J_m^2(k_r^{mn}a)}{(k_r^{mn}a)^2} + J_m'^2(k_r^{mn}a) \right]^{1/2}, \tag{12}$$

$$D_{mn}(\tau) = \frac{k^2 a}{(k_r^{mn})^2 - \tau^2 k^2} [k\tau J_m(k_r^{mn}a) J'_m(\tau ka) - k_r^{mn} J'_m(k_r^{mn}a) J_m(\tau ka)]. \tag{13}$$

Eq. (11) shows the incident modes can be coupled with other reflection modes. And it can be simplified as

$$Z'_{mnl} = \frac{1}{W} \int_0^{\infty} \frac{\tau^3 J_m'^2(\tau ka) - 2\mathrm{i}\beta\tau^2 J_m(\tau ka) J'_m(\tau ka) - \beta^2 \tau J_m^2(\tau ka)}{\sqrt{1-\tau^2}(\tau^2 - (k_r^{mn})^2/k^2)(\tau^2 - (k_r^{ml})^2/k^2)}\, \mathrm{d}\tau \tag{14}$$

with

$$W = \frac{1}{2} \left[\left(1 - \left(\frac{\beta k}{k_r^{mn}} \right)^2 - \frac{m^2}{(k_r^{mn}a)^2} \right) \right]^{1/2} \left[\left(1 - \left(\frac{\beta k}{k_r^{ml}} \right)^2 \right) - \frac{m^2}{(k_r^{ml}a)^2} \right]^{1/2}. \tag{15}$$

The above integral can be split into two parts over the range (0,1) and (1, ∞) and with the changes of variable $\tau = \sin\phi$ and $\tau = \cos\xi$ in those respective ranges, the impedance equation becomes

$$\begin{aligned} Z'_{mnl} = {} & \frac{1}{W} \int_0^{\pi/2} \frac{\sin^3\phi J_m'^2(ka\sin\phi) - 2\mathrm{i}\beta\sin^2\phi J_m(ka\sin\phi) J'_m(ka\sin\phi) - \beta^2 \sin\phi J_m^2(ka\sin\phi)}{(\sin^2\phi - (k_r^{mn})^2/k^2)(\sin^2\phi - (k_r^{ml})^2/k^2)}\, \mathrm{d}\phi \\ & + \frac{\mathrm{i}}{W} \int_0^{\infty} \frac{\cosh^3\xi J_m'^2(ka\cosh\xi) - 2\mathrm{i}\beta\cosh^2\xi J_m(ka\cosh\xi) J'_m(ka\cosh\xi) - \beta^2 \cosh\xi J_m^2(ka\cosh\xi)}{(\cosh^2\phi - (k_r^{mn})^2/k^2)(\cosh^2\phi - (k_r^{ml})^2/k^2)}\, \mathrm{d}\xi. \end{aligned} \tag{16}$$

Eq. (16) is actually the expression of calculation of self-radiation impedance for a finite cylindrical duct. When $n = l$, Z'_{mnl} is called the direct self-radiation impedance; when $n \neq l$, Z'_{mnl} is called the coupling self-radiation impedance.

2.3. Mutual impedance

Considering an opening interface in the one side of the duct is a source whose vibration generates sound and it propagates to the other side producing the pressure force. The axial velocity distribution on the interface at this opening of a finite cylindrical duct (suppose at the left side, $x = -L$) can be expressed in terms of the sum of acoustic modes in the circular cross-section:

$$u_x(r,\theta,-L) = -\frac{\mathrm{i}}{\rho\omega}\frac{\partial p}{\partial x}\bigg|_{x=-L} = \sum_{m=-\infty}^{m=\infty} \mathrm{e}^{-\mathrm{i}m\theta} \sum_{n=1}^{\infty} U_{mn} J_m(k_r^{mn} r). \tag{17}$$

The pressure inside the duct can be written as

$$p(r,\theta,x) = \sum_{m=-\infty}^{\infty} \mathrm{e}^{-\mathrm{i}m\theta} \sum_{n=1}^{\infty} C_{mn} J_m(k_r^{mn} r) \mathrm{e}^{\mathrm{i}k_x^{mn} x}, \tag{18}$$

where C_{mn} is a mode coefficient. The pressure should satisfy the boundary condition at the interference

$$C_{mn} = \frac{\rho k c U_{mn}}{k_x^{mn}} \mathrm{e}^{\mathrm{i}k_x^{mn} L}. \tag{19}$$

Thus, the pressure of the sound field at the (m, n) mode is

$$p(r,\theta,x) = \rho k c \sum_{m=-\infty}^{\infty} \mathrm{e}^{-\mathrm{i}m\theta} \sum_{n=1}^{\infty} \frac{U_{mn}}{k_x} \mathrm{e}^{\mathrm{i}k_x^{mn} L} \mathrm{e}^{-\mathrm{i}k_x^{mn} x} J_m(k_r^{mn} r). \tag{20}$$

In acoustics the radiation impedance is often defined as the ratio of a force to a velocity, but the impedance defined by the radiation power is more generally useful. Based on the definition of mutual radiation impedance for two radiators [16], the mutual impedance of the two open ends could be written as

$$Z'' = \frac{1}{\bar{U}_1 \bar{U}_2^*} \int_{S_2} p_1^{S_2} u_2^* \, \mathrm{d}S, \tag{21}$$

where U_1 and U_2 are the amplitude of the velocity at the open ends of left and right sides, respectively (the velocity of both open ends is assumed to have the same amplitude and be in phase because they are symmetric to center plane $x = 0$); * is the complex conjugate; $p_1^{S_2}$ is the pressure on the right open end (S_2) produced by the vibration at the interface of the left end (S_1); u_2 is the velocity distribution on the right end.

$$Z''_{mnl} = \frac{1}{U_1^{ml} U_2^{mn*}} \int_{S_2} p_1^{ml} u_2^{mn*} \mathrm{d}S = \frac{\rho k c}{k_x^{ml}} \mathrm{e}^{\mathrm{i}2k_x^{ml} L} \int_0^{2\pi} \mathrm{d}\theta \int_0^a J_m(k_r^{ml} r) J_m(k_r^{mn} r) r \, \mathrm{d}r. \tag{22}$$

From the result of the integration and the orthogonal property of the product of Bessel functions [21], the above formula can be simplified to

$$Z''_{mnl} = \begin{cases} \dfrac{\pi\rho kca^2}{k_x^{mn}} e^{i2k_x^{mn}L}[J_m(k_r^{mn}a)^2 - J_{m-1}(k_r^{mn}a)J_{m+1}(k_r^{mn}a)], & (n = l), \\ 0, & (n \neq l). \end{cases} \tag{23}$$

The total radiation impedance can be expressed as [16]

$$Z_{mnl} = Z'_{mnl} + Z''_{mnl}\frac{U_1^{mn}}{U_2^{mn}} = Z'_{mnl} + Z''_{mnl}. \tag{24}$$

Thus, the sound field of the finite ducts can be calculated in terms of acoustic modes by Eq. (10), replacing Z'_{mnl} by Z_{mnl}.

3. Numerical results and discussions

The finite cylindrical duct model used here is a duct with half-length $L = 0.6\,\text{m}$ and radius $a = 0.3\,\text{m}$. The results for three situations of the acoustic boundary condition of the wall: rigid, acoustic admittance $\beta = 0.1 + 0.1\text{i}$ and $\beta = 1 + 1\text{i}$, will be presented in this section. Before the calculation for self-radiation and mutual radiation impedances, the wavenumbers for different radial modes satisfying the three boundary conditions should be found.

3.1. Wavenumbers for radial modes

For the hard wall (rigid boundary), the wavenumbers can be found from solutions of the equation $\text{d}[J_m(k_r r)]/\text{d}(k_r r) = 0$. Then the cut-off frequencies can be obtained by letting $k_x^{mn} = 0$, thus $k_{\text{cut-off}} = k_r^{mn}$. Table 1 shows the cut-off frequencies in Hz for the model in this study .

For the wall with acoustic admittances $\beta = 0.1 + 0.1\text{i}$ and $\beta = 1 + 1\text{i}$, the Newton method [22] is used to find the roots for Eq. (6). The procedure is iterated as

$$y_{n+1} = y_n - \frac{f(y_n)}{f'(y_n)}, \tag{25}$$

where

$$f(y_n) = y_n J_{m-1}(y_n) - mJ_m(y_n) - \text{i}\beta kaJ_m(y_n), \tag{26}$$

Table 1
Cut-off frequencies $k_{\text{cut-off}}$ in Hz corresponding to radial acoustic modes k_r^{mn}

n	$m = 0$	$m = 1$	$m = 2$	$m = 3$	$m = 4$
1	0	332	550	757	956
2	691	961	1210	1443	1674
3	1266	1540	1798	2047	2287
4	1834	2112	2375	2632	2879

$$f'(y_n) = J_{m-1}(y_n) + 0.5y_n[J_{m-2}(y_n) - J_m(y_n)] - 0.5m[J_{m-1}(y_n) - J_{m+1}(y_n)] - \mathrm{i}0.5\beta ka[J_{m-1}(y_n) - J_{m+1}(y_n)]. \quad (27)$$

The initial value for this iteration is given by Eq. (7) with a smaller admittance value to improve the convergent speed of the iteration procedure. For instance, bringing $\beta = 0.01 + 0.01\mathrm{i}$ and $\beta = 0.1 + 0.1\mathrm{i}$ into Eq. (7) to generate initial values for solutions of $\beta = 0.1 + 0.1\mathrm{i}$ and $\beta = 1 + 1\mathrm{i}$, respectively.

3.2. Self-radiation impedance

Based on Eqs. (14) and (16), the self-radiation impedances for modes $m = 0, 1$ and $n = 1, 2, 3$ with a frequency range from 0 to 2000 Hz are presented. As $z \to \infty, J_m(z) \to 0$, the infinite integral in Eq. (16) is convergent. For the rigid boundary condition ($\beta = 0$), $\tau = k_r^{mn}/k$ ($n = l$) are the simple poles for expressions in the integral, and it can be rewritten as ($\tau = \sin\phi$ or $\tau = \cosh\xi$)

$$\left.\frac{\tau^3 J_m'^2(\tau ka)}{(\tau^2 - (k_r^{mn})^2/k^2)(\tau^2 - (k_r^{ml})^2/k^2)}\right|_{\tau = k_r^{mn}/k} = \frac{ka^2 J_m^2(k_r^{mn}a)}{4k_r^{mn}}\left[1 - \left(\frac{m}{k_r^{mn}}\right)^2\right]^2. \quad (28)$$

The generalized direct self-radiation impedances Z'_{mnl} ($n = l$) for $m = 0$ and $n = 1, 2, 3$ are shown in Figs. 3, 4, and 5 respectively. Their real and imaginary parts are plotted. Similar to the definition for the specific acoustic impedance [23], the real and imaginary parts represent the resistive and reactive components of impedances, respectively. These figures show a common

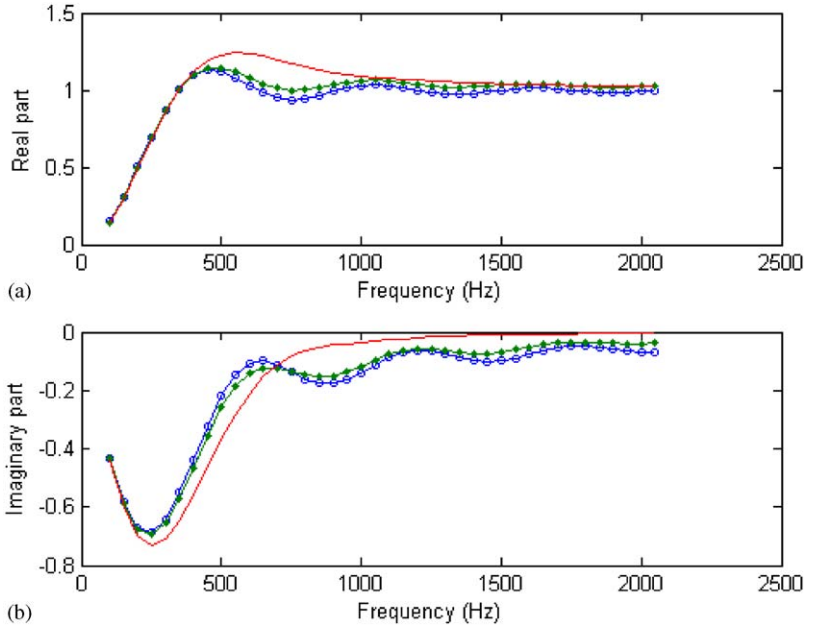

Fig. 3. Generalized direct self-radiation impedance Z'_{011} ($m = 0, n = l = 1$, plane wave) (a) real part and (b) imaginary part for the duct wall with admittance values: $\beta = 0$ (rigid), —□—; $\beta = 0.1 + 0.1i$, —+—; $\beta = 1 + 1i$, ——.

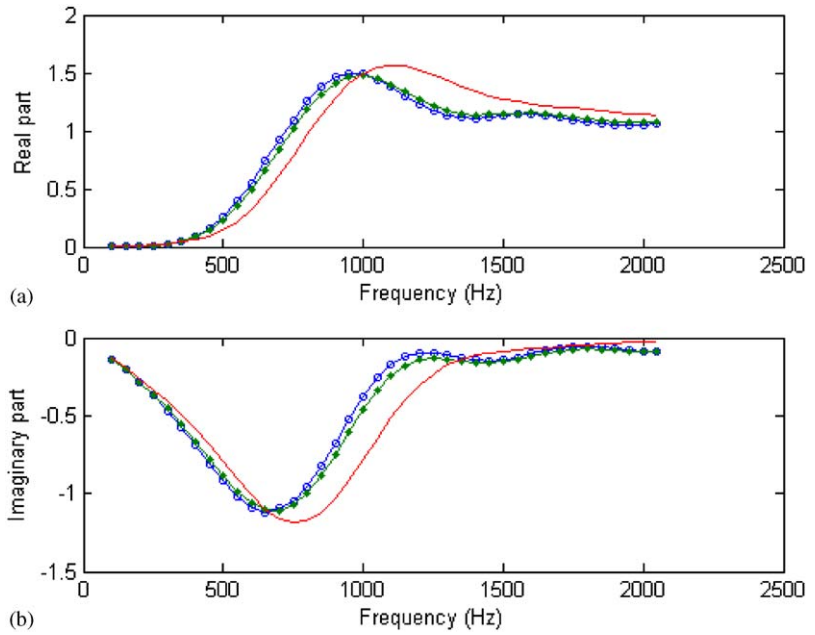

Fig. 4. Generalized direct self-radiation impedance Z'_{022} ($m = 0$, $n = l = 2$) (a) real part and (b) imaginary part for the duct wall with admittance values: key as in Fig. 3.

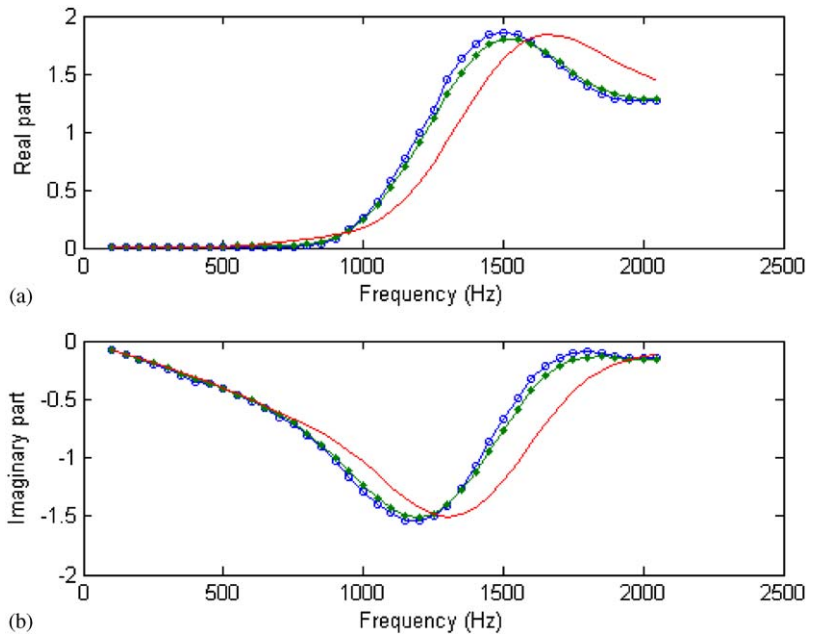

Fig. 5. Generalized direct self-radiation impedance Z'_{033} ($m = 0$, $n = l = 3$) (a) real part and (b) imaginary part for the duct wall with admittance values: key as in Fig. 3.

trend, in that the largest values of the impedances are increased in amplitude and move to higher frequency at higher modes compared to the lower modes (more accurately, compared by their cut-off frequency). The real part (resistance) of the impedance is a measure of the radiation efficiency for the corresponding incident mode at the open ends. This indicates that the interface of the duct open ends will be a good radiator for a certain acoustic mode just over its corresponding cut-off frequency and the higher mode waves will more easily radiate out the duct compared to the lower mode waves. In other words, incident waves with lower modes are generally of higher reflection coefficients at the open end of the duct than the higher mode waves. Fig. 3 shows the real part of the impedances for the plane wave is relatively small at low frequency and converge to unity at higher frequency. Both the real and imaginary parts of the impedance have small oscillations at higher frequency (>500 Hz), but this does not happened for the walls with large admittance ($\beta = 1 + 1\mathrm{i}$). It is also true in Figs. 4 and 5 that the real part of the impedances are near zero at low frequency and increase gradually as the frequency increases over the cut-off frequency of the corresponding mode. After passing the largest value (absolute value for the imaginary part), the real part approaches unity and the imaginary part is close to zero.

It is obvious that the curves of the impedance for the walls with admittance $\beta = 0$ and $\beta = 0.1 + 0.1\mathrm{i}$ are similar in general shape at all frequency ranges whereas they are quite different from the admittance $\beta = 1 + 1\mathrm{i}$ at intermediate frequencies. For instance, the real part of the impedance for $\beta = 1 + 1\mathrm{i}$ is larger than the other two cases in the frequency range from 500 to 1000 Hz in Fig. 3 and 500 to 1500 Hz in Fig. 4. This frequency range is expanded as the mode number is increased. The imaginary parts show similar features. Figs. 6–8 show Z'_{mnl} $(n = l)$ for $m = 1$ and $n = 1, 2, 3$ respectively and the impedances in these figures possess the same features as those found in Figs. 3–5.

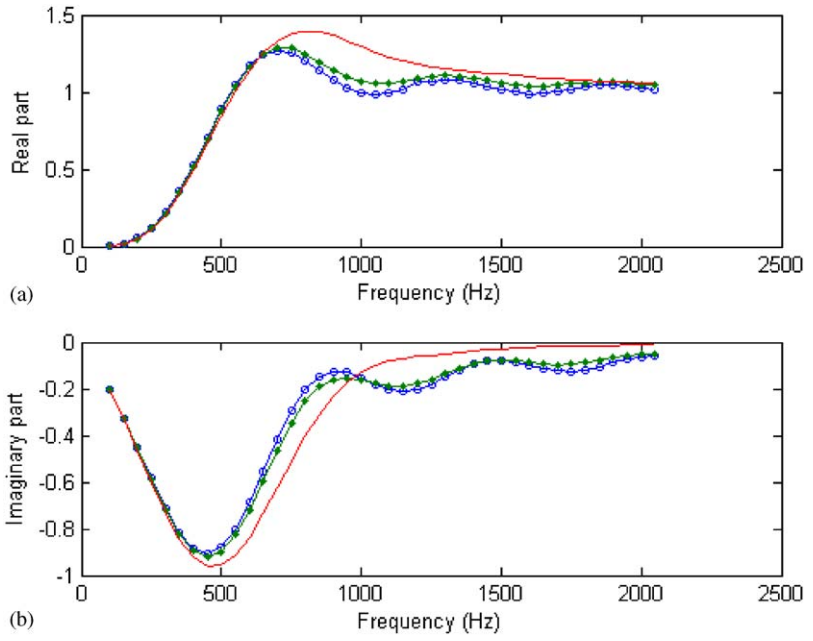

Fig. 6. Generalized direct self-radiation impedance Z'_{111} ($m = 1$, $n = l = 1$) (a) real part and (b) imaginary part for the duct wall with admittance values: key as in Fig. 3.

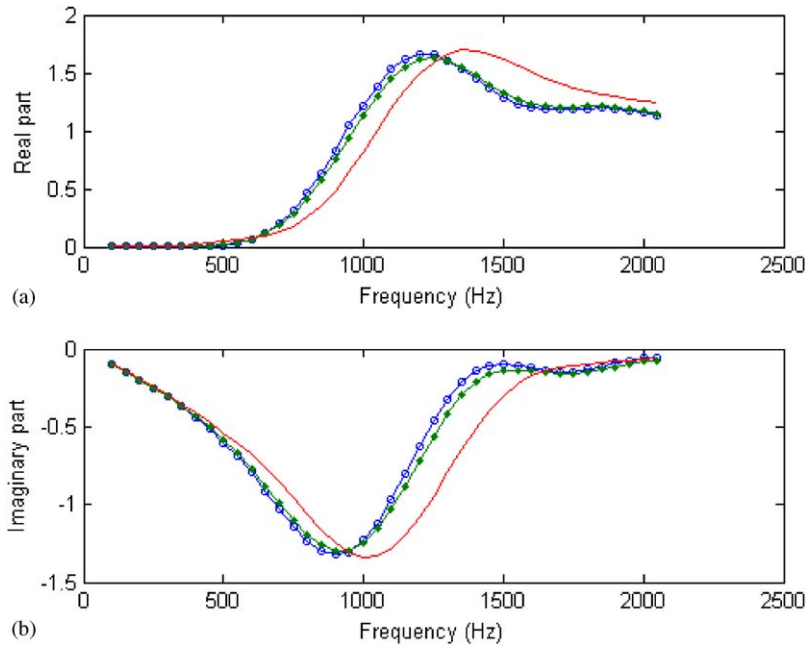

Fig. 7. Generalized direct self-radiation impedance Z'_{122} ($m = 1$, $n = l = 2$) (a) real part and (b) imaginary part for the duct wall with admittance values: key as in Fig. 3.

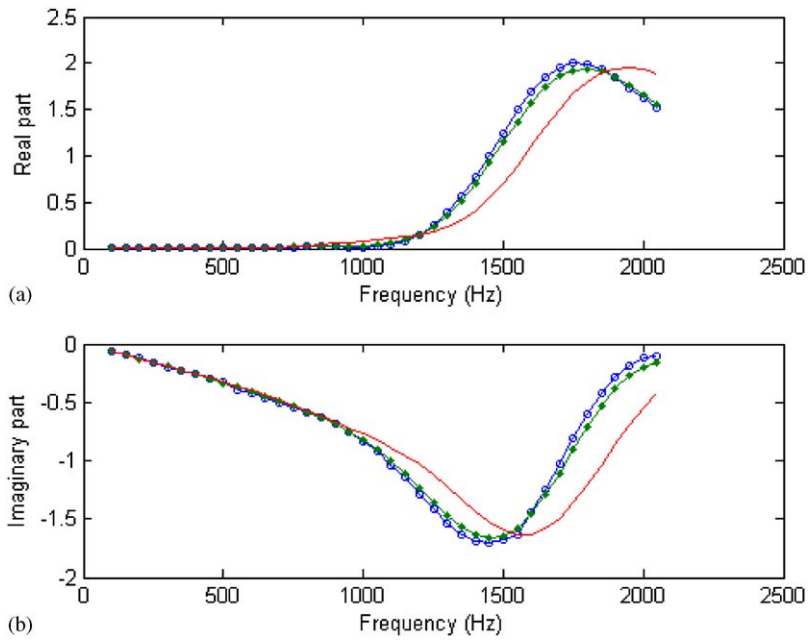

Fig. 8. Generalized direct self-radiation impedance Z'_{133} ($m = 1$, $n = l = 3$) (a) real part and (b) imaginary part for the duct wall with admittance values: key as in Fig. 3.

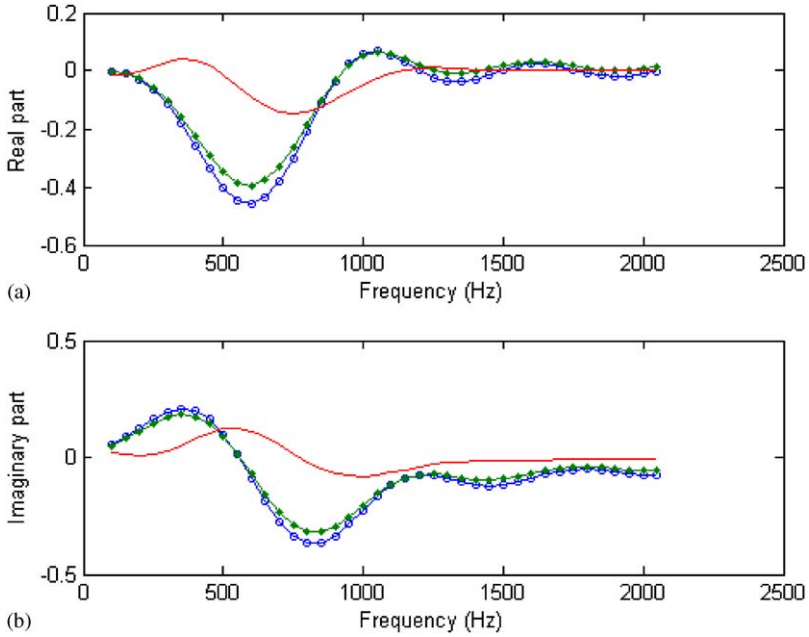

Fig. 9. Generalized coupling self-radiation impedance Z'_{021} ($m = 0, n = 2$ and $l = 1$) (a) real part and (b) imaginary part for the duct wall with admittance values: key as in Fig. 3.

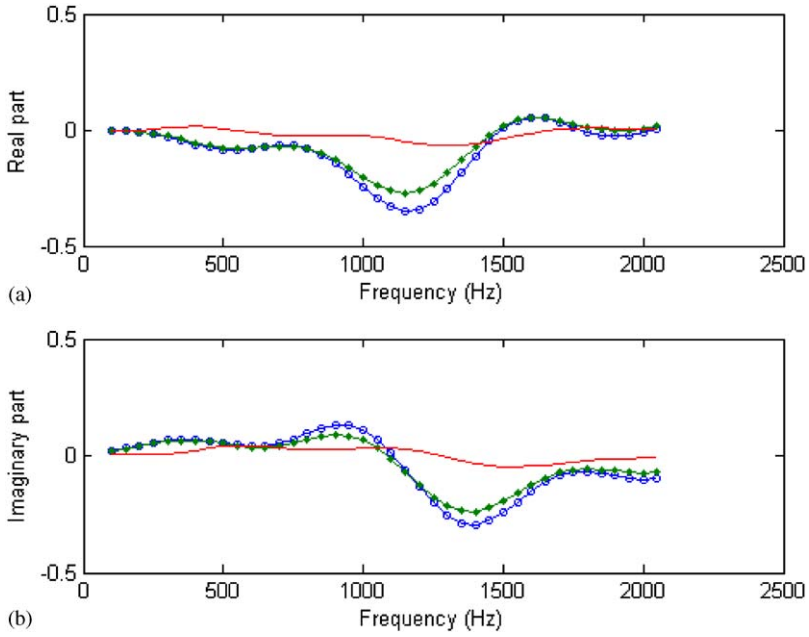

Fig. 10. Generalized coupling self-radiation impedances Z'_{031} ($m = 0, n = 3$ and $l = 1$) (a) real part and (b) imaginary part for the duct wall with admittance values: key as in Fig. 3.

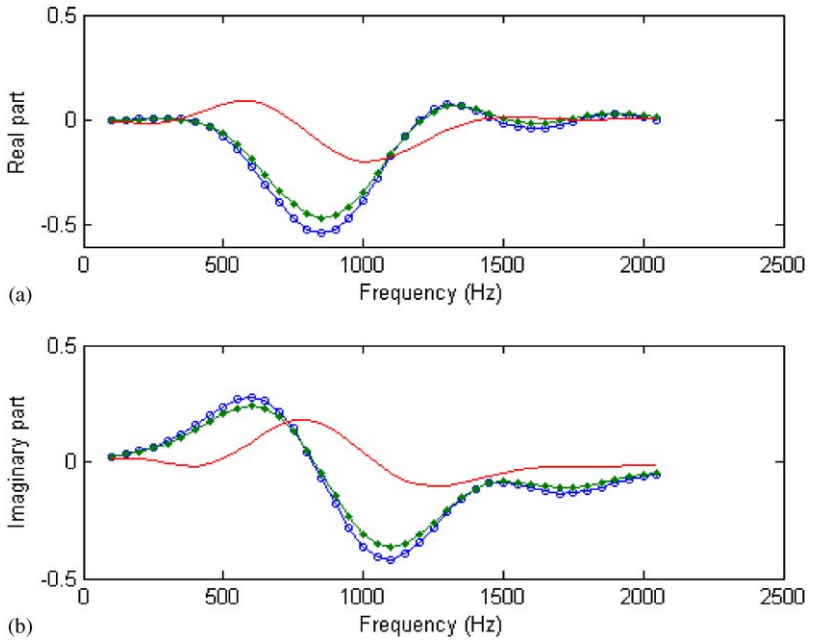

Fig. 11. Generalized coupling self-radiation impedances Z'_{121} ($m = 1, n = 2$ and $l = 1$) (a) real part and (b) imaginary part for the duct wall with admittance values: key as in Fig. 3.

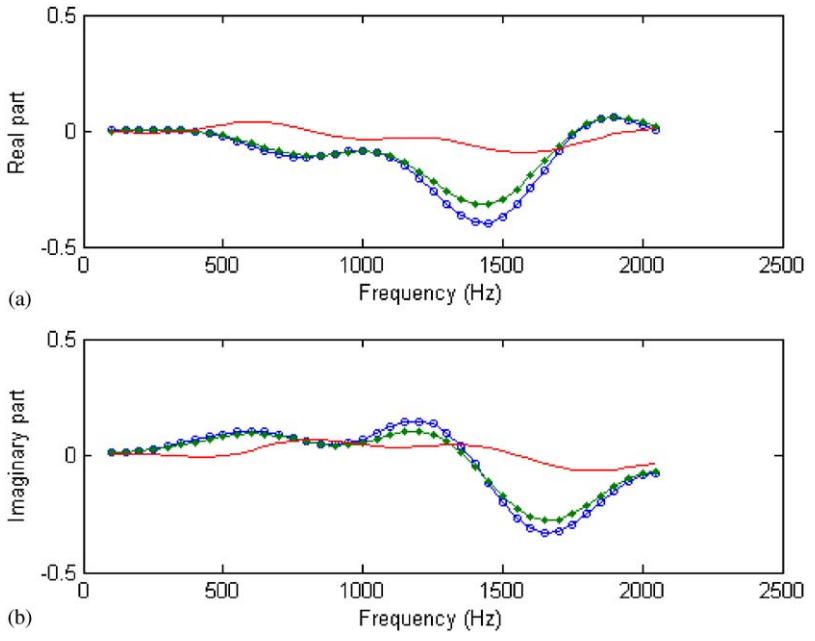

Fig. 12. Generalized coupling self-radiation impedances Z'_{131} ($m = 1, n = 3$ and $l = 1$) (a) real part and (b) imaginary part for the duct wall with admittance values: key as in Fig. 3.

Distinct from the direct self-radiation impedance, $Z'_{mnl}$is called the coupling self-radiation impedance when $n \neq l$. Figs. 9–12 show the coupling impedances for several modes. The coupling Z'_{mnl} indicates the nth radial pressure distribution generated by the lth radial velocity distribution at the opening. It was found that the largest values of these coupling impedances are smaller than those of the direct impedances. This means that the influence of other modes on the radiation impedance is not as strong as that caused by itself. The amplitude for the wall with large admittance $\beta = 1 + 1\mathrm{i}$ is small, especially when n and l are far apart (see Figs. 10,11 for Z'_{031} and Z'_{131}). It may be concluded that the coupling factor for the large admittance can be ignored when the two modes (n and l) are not contiguous. The largest amplitude of the coupling impedance normally appears at the vicinity of the cut-off frequency (see Table 1).

3.3. Mutual radiation impedance

The self-radiation impedance for the finite duct is the same as the total radiation impedance of the semi-infinite duct. Due to the acoustic interaction of the two open ends of finite ducts, their mutual impedance should be investigated. Figs. 13–16 show the mutual impedance Z''_{mnl} for some modes. The plane wave shows the largest mutual interaction and this effect decreases as the mode number is increased. The value of the impedance is decreased as the wall admittance is increased because the absorptive wall attenuates the sound wave propagation in the duct, thus the acoustic interaction is reduced between the two ends. Referring to Eq. (23), it can be found that the amplitude of the mutual impedances is proportional to the area of duct terminations.

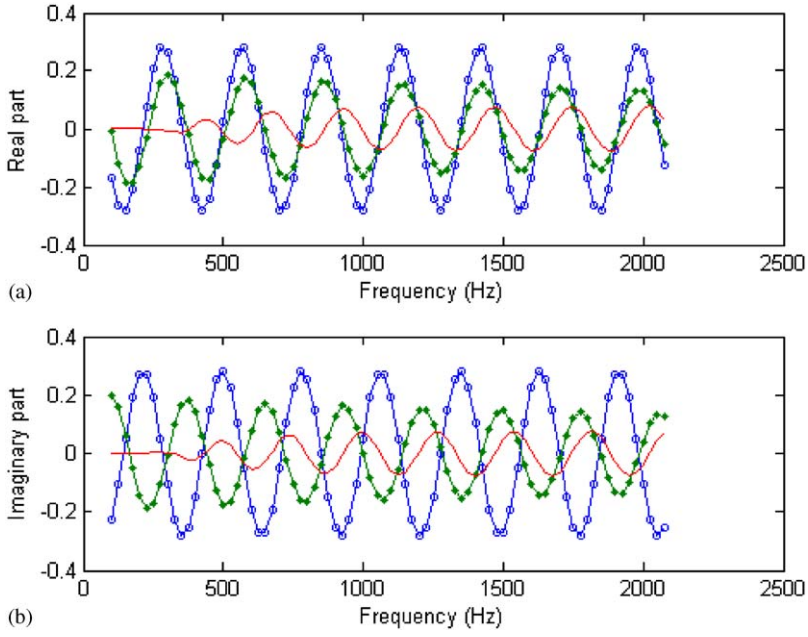

Fig. 13. Mutual radiation impedance Z''_{011} ($m = 0, n = l = 1$) (a) real part and (b) imaginary part for the duct wall with admittance values: key as in Fig. 3.

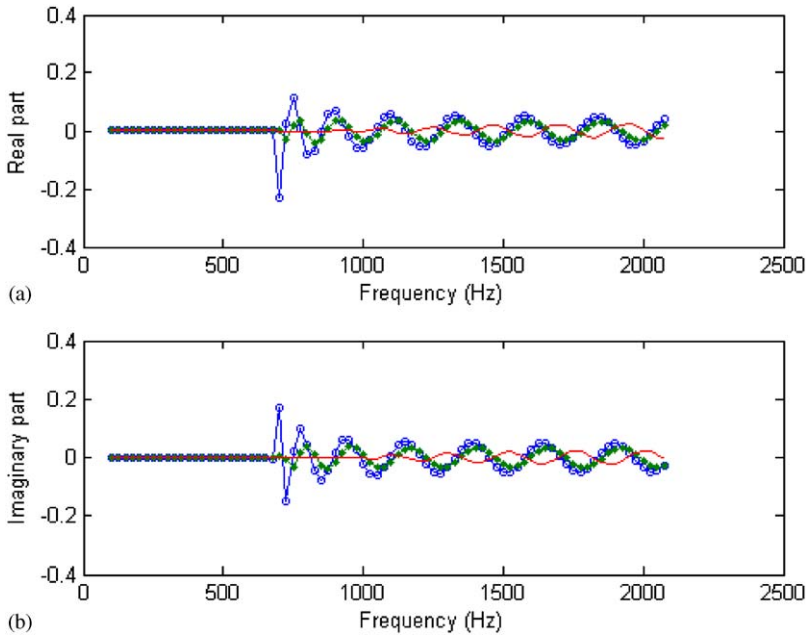

Fig. 14. Mutual radiation impedance Z''_{022} ($m = 0, n = l = 2$) (a) real part and (b) imaginary part for the duct wall with admittance values: key as in Fig. 3.

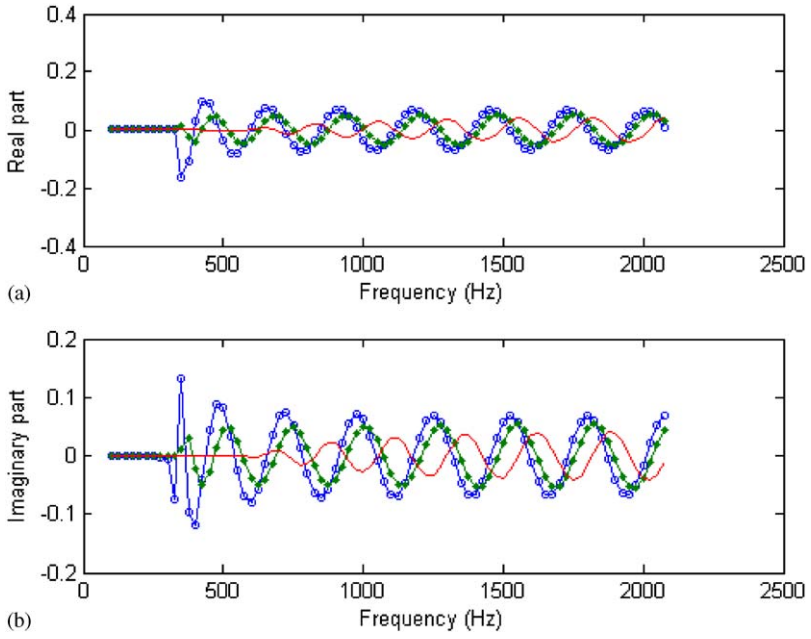

Fig. 15. Mutual radiation impedance Z''_{111} ($m = 1, n = l = 1$) (a) real part and (b) imaginary part for the duct wall with admittance values: key as in Fig. 3.

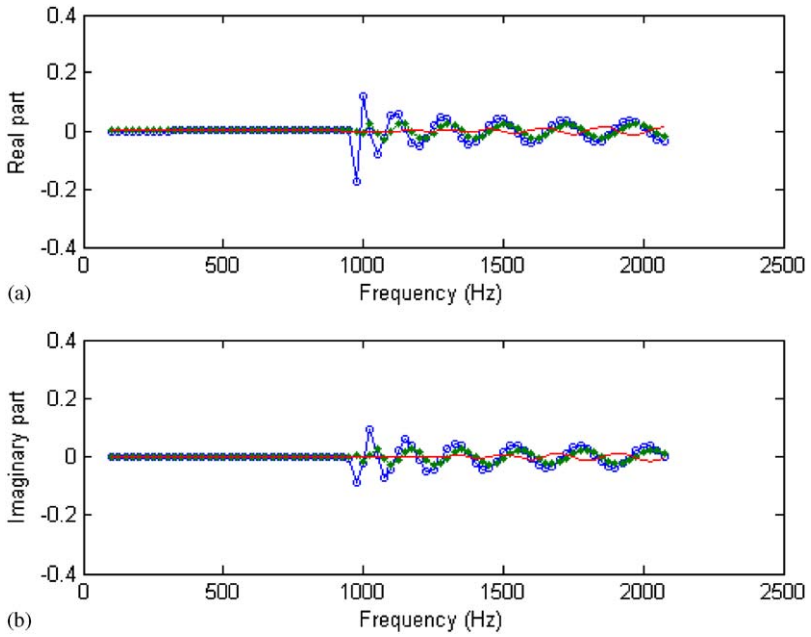

Fig. 16. Mutual radiation impedance Z''_{122} ($m = 1, n = 1 = 2$) (a) real part and (b) imaginary part for the duct wall with admittance values: key as in Fig. 3.

Theoretically there is no attenuation of the propagation for the acoustic mode waves (over the corresponding cut-off frequencies) in the duct with a rigid wall, therefore the amplitude of the mutual impedance is independent of the duct length in this situation. However, the amplitude value will decrease as the duct length is increased for the duct with an acoustical absorptive wall.

From Figs. 14–16, it can be seen that the mutual impedance is zero at low frequency ($<$ the cut-off frequency) because the axial wavenumber k_x^{mn} is imaginary and the waves decay quickly and little sound energy can reach the other side of the duct. At the cut-off frequency, the amplitude of impedances increases dramatically and oscillates around zero with a small amplitude after it passes the cut-off frequency. It seems that the higher frequency waves can more easily propagate in the duct with a large admittance wall than lower frequency waves because the amplitude of the impedances for the duct wall with $\beta = 1 + 1\mathrm{i}$ are slowly increased as the frequency is increased. This phenomena is caused by the term $\mathrm{e}^{\mathrm{i}2k_x^{mn}L}$ in Eq. (23) where the value of the imaginary part of the axial wavenumber k_x^{mn} for the absorptive duct wall is a little diminished as the frequency is increased. As a result, the higher frequency modes are comparatively less attenuated by the term k_x^{mn} than the lower frequency modes.

4. Conclusions

The mathematical expressions of acoustical radiation impedance for flanged finite cylindrical ducts with hard- and absorptive-walls have been presented. The acoustical interaction between the two open ends of the ducts has been investigated. Calculations for the self-radiation and mutual

impedances for several modes show some useful results. The largest value of the self-radiation impedance increases and moves to a higher frequency as the corresponding cut-off frequency is increased; the coupling factor for the ducts with large admittance walls could be ignored; the mutual interference between two open ends is greater for the plane wave than that of other higher modes.

A deep understanding of the radiation impedance for the finite cylindrical ducts is very important, because it provides the theoretical possibility for the simulation of the sound fields inside ducts, which could be used to describe sound radiation characteristics of the gradient coils in MRI scanners.

References

[1] S.A. Counter, A. Olofsson, E. Borg, B. Bjelke, A. Haggstrom, H.F. Grahn, Analysis of magnetic resonance imaging acoustic noise generated by a 4.7 T experimental system, *Acta Otolaryngolica* 120 (2000) 739–743.

[2] R.E. Brumment, J.M. Talbot, P. Charuhas, Potential hearing loss resulting from MR imaging, *Radiology* 169 (1988) 539–540.

[3] C.K. Mechefske, Y. Wu, B.K. Rutt, MRI gradient coil cylinder sound field simulation and measurement, *Journal of Biomechanical Engineering* 124 (2002) 1–6.

[4] A. Kuijpers, S.W. Rienstra, G. Verbeek, J.W. Verheij, The acoustic radiation of baffled finite ducts with vibrating walls, *Journal of Sound and Vibration* 216 (1998) 461–493.

[5] F. Fahy, *Sound and Structural Vibration: Radiation, Transmission and Response*, Academic Press; London, 1987; 2000 re-issue.

[6] P.M. Morse, K. Unoingard, *Theoretical Acoustics*, Princeton University Press, Princeton, 1986.

[7] P.E. Doak, Excitation transmission and radiation of sound from a source in a hard-walled duct of finite length—I: the effects of duct cross-section geometry and source distribution space–time pattern, *Journal of Sound and Vibration* 31 (1973) 1–72.

[8] P.E. Doak, Excitation, transmission and radiation of sound from a source in a hard-walled duct of finite length—II: the effects of duct length, *Journal of Sound and Vibration* 31 (1973) 137–174.

[9] P.M. Morse, *Vibration and Sound*, second ed., McGraw-Hill, New York, 1948.

[10] L.B. Felsen, H.Y. Yee, Ray method for sound-wave reflection in an open-ended circular pipe, *The Journal of the Acoustical Society of America* 44 (1968) 1028–1039.

[11] C.L. Morfey, A note on the radiation efficiency of acoustic duct modes, *Journal of Sound and Vibration* 9 (3) (1969) 367–372.

[12] W.E. Zorumski, Generalized radiation impedances and reflection coefficients of circular and annular ducts, *The Journal of the Acoustical Society of America* 54 (1973) 1667–1673.

[13] R.L. Pritchard, Mutual acoustic impedance between radiators in an infinite rigid plane, *The Journal of the Acoustical Society of America* 32 (1960) 730–737.

[14] C.H. Sherman, Mutual radiation impedance of sources on a sphere, *The Journal of the Acoustical Society of America* 31 (1959) 947–951.

[15] J.E. Greenspon, C.H. Sherman, Mutual-radiation impedance and nearfield pressure for pistons on a cylinder, *The Journal of the Acoustical Society of America* 36 (1964) 149–152.

[16] K.C. Chan, Mutual acoustic impedance between flexible disks of different sizes in an infinite rigid plane, *The Journal of the Acoustical Society of America* 42 (1967) 1060–1063.

[17] W. Thompson Jr., The computation of self- and mutual-radiation impedances for annular and elliptical pistons using Bouwkamp's integral, *Journal of Sound And Vibration* 93 (1971) 221–233.

[18] G.W. Johnston, K. Oginoto, Sound radiation from a finite-length unflanged circular duct with uniform axial flow—II: computed radiation characteristics, *The Journal of the Acoustical Society of America* 68 (1980) 1871–1883.

[19] K.S. Wang, T.C. Tszeng, Propagation and radiation of sound in a finite length duct, *Journal of Sound and Vibration* 93 (1984) 57–79.
[20] P.O.A.L. Davis, Waveguides, in: M. Crocker (Ed.), *Handbook for Acoustics*, Wiley, New York, 1998, pp. 83–96 (Chapter 7).
[21] G.N. Watson, *A Treatise on the Theory of Bessel Functions*, second ed., Cambridge University Press, Cambridge, 1966.
[22] A.L. Garcia, *Numerical Methods for Physics*, second ed., Prentice-Hall, Englewood Cliffs, 2000.
[23] F. Fahy, *Foundations of Engineering Acoustics*, Academic Press, London, 2001.